Colloids and Surfaces A 553 (2018) 397–405

Contents lists available at ScienceDirect

Colloids and Surfaces A

journal homepage: www.elsevier.com/locate/colsurfa

Enhanced adsorption of anionic surfactants on negatively charged quartz sand grains treated with cationic polyelectrolyte complex nanoparticles

Xilong Zhou, Jenn-Tai Liang, Corbin D. Andersen, Jiajia Cai, Ying-Ying Lin*

Petroleum Engineering, Texas A&M University, College Station, TX 77843-3116, United States

GRAPHICAL ABSTRACT

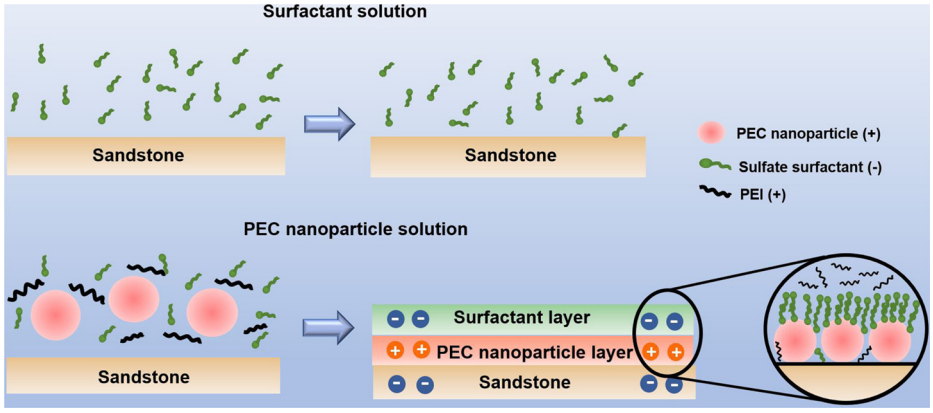

ARTICLE INFO

Keywords:
Surfactant
Nanoparticle
Polyelectrolyte complex
Adsorption
QCM-D
EOR

ABSTRACT

The objective of this study is to examine the potential of using polyelectrolyte complex (PEC) nanoparticles to enhance the adsorption of anionic surfactants on negatively charged surface of quartz sand grains. The hypothesis is that a cationic PEC layer formed on the negatively charged quartz surface can enhance the adsorption of anionic surfactants on quartz sand grains. Both static adsorption tests and a quartz crystal microbalance with dissipation monitoring (QCM-D) were used to test the hypothesis. We measured the rate and extent of adsorption of an anionic sulfate surfactant onto bare quartz sand grains versus sand grains pre-treated with PECs. Total organic carbon (TOC) and total nitrogen (TN) analyses were used to quantitatively measure the adsorption of surfactant and PECs. Real-time adsorption monitoring was performed on silica model surfaces by QCM-D. Consistent with our hypothesis, the results showed that the level of adsorption of the anionic sulfate surfactant on PEC treated quartz sand grains (21.5 mg/g of sand) was indeed significantly higher than that on bare untreated sand grains (negligible adsorption). Our results also confirmed a proposed four-stage adsorption mechanism for the enhanced adsorption of anionic surfactants on negatively charged quartz sand grains treated with PEC nanoparticles.

Abbreviations: DI, deionized water; PEC, polyelectrolyte complex; DLVO, Derjaguin-Landau-Verwey-Overbeek; EOR, enhanced oil recovery; EE, entrapment efficiency; QCM-D, quartz crystal microbalance with dissipation; TC, total carbon; TN, total nitrogen; TOC, total organic carbon

* Corresponding author.
E-mail address: yylin@tamu.edu (Y.-Y. Lin).

https://doi.org/10.1016/j.colsurfa.2018.05.079
Received 4 April 2018; Received in revised form 24 May 2018; Accepted 27 May 2018
Available online 28 May 2018

1. Introduction

Surfactants are extensively used in today's world and have applications in nearly every industry, e.g. oil recovery, detergency, corrosion inhibition, mineral flotation, dispersion of solids, etc. [1]. Surfactants have been used in the oil industry for many years to enhance oil recovery by removing residual oil trapped in reservoir rock through interfacial tension (IFT) reduction and wettability alteration [2]. By lowering the IFT between oil and water, the capillary force is lessened to such an extent that entrapped oil can be mobilized and produced [3,4]. With regards to wettability, adsorption of surfactants on rock surface can alter the affinity of the rock surface to formation fluids. Under the right circumstances, this can improve oil recovery through enhanced spontaneous imbibition of the injected water that displaces oil from the reservoir rock [5].

The adsorption of surfactants at the solid/solution interface has numerous applications and has been studied extensively [6–9]. It is known that this interaction depends on three factors [10]: the characteristics of the solid, the properties of the surfactant, and the conditions of the environment. In the oil and gas industry, numerous studies have been conducted on the surface charges of reservoir rocks to understand the mechanisms of adsorption and their impacts on hydrocarbon recovery [1,11,12]. As expected, electrostatic interactions are the primary driving force. In other words, in order to promote surfactant adsorption on a rock surface that carries a surface charge, the surfactant must carry the opposite charge. However, in oil recovery applications, anionic surfactants are often preferred over cationic surfactants because the lower cost [13,14]. Therefore, there is an incentive to find a way to enhance the adsorption of anionic surfactant on negatively charged sandstone reservoir rock.

PEC nanoparticles are an arrangement of poly-ionic species formed through electrostatic interactions. The properties of these complexes have been reviewed by Berger et al. [15]. PECs have numerous potential applications across many industries including drug delivery [16], waste water treatment, mining, paper production, cosmetics, and detergents [17]. They have also demonstrated utility in the oil industry for fracture fluid cleanup [18,19], delayed gelation of diverting agents [20], and long-term controlled release of cross linkers [21,22].

Similar to surfactants, the adsorption of PECs onto solid surfaces has been well documented in literature. Reihs et al. [23,24] studied the adsorption behavior of PEC particles onto silica, taking into consideration surface pretreatment, polyanion selection, pH, and centrifugation. They noted that PEC refinement through centrifugation resulted in stronger adsorption to the mineral's surface. They concluded that, without refinement, unentrapped polymers compete with PECs for active sites on the negatively charged silica. Using a quartz crystal microbalance with dissipation (QCM-D) and atomic-force microscopy (AFM), Ondaral et al. compared the adsorption processes of PECs comprised of both high and low molecular weight polymers. One of their interesting findings was that certain PECs first adsorb and then deform with time on the surface. The cause of the observed deformation was thought to result from migrating electrolytes through the adsorbed PEC layers [25].

Yanez et al. [26] studied the adsorption of surfactants in the presence of dendrimers. They noted a significant difference between the adsorption of a premixed dendrimer/surfactant solution to that of a system consisting of pre-adsorbed dendrimers followed by the surfactant. This result, they explained, suggests that dendrimers can be used to control the delivery rate of species to the surface interface. Gao et al. [27,28] studied the adsorption of surfactant entrapping PECs onto gold and silica sensors using QCM-D and discussed the effects of salinity on adsorption. Furthermore, a sodium dodecyl sulfate-entrapping PEC was developed and its interfacial properties were studied by measuring surface tension and interfacial microrheology. The disassembly of PECs into their components, triggered by interactions at the phase interface, was observed. This suggests that PECs may be used for the delivery and delayed release of surfactants at the fluid/fluid interface.

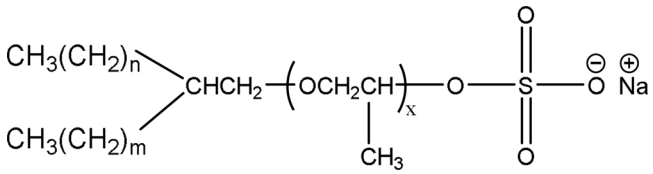

Fig. 1. Molecular structure of an Alcohol Propoxy Sulfate (APS) courtesy of Ref. [3].

In this study, we examine the potential of using polyelectrolyte complex (PEC) nanoparticles to enhance the adsorption of anionic surfactants on negatively charged surface of quartz sand grains. We hypothesize that a cationic PEC layer formed on the negatively charged quartz surface can enhance the adsorption of anionic surfactants on quartz sand grains. Both static adsorption tests and a quartz crystal microbalance with dissipation monitoring (QCM-D) will be used to test the hypothesis. Results from these tests will also be used to confirm a proposed four-stage mechanism for the enhanced anionic surfactant adsorption on quartz sand grains coated with PEC nanoparticles.

2. Experimental section

2.1. Materials

The Alcohol Propoxy Sulfate (APS) surfactant (C12-13, 7 propylene oxide and a sulfate group) used in this study was a commercial surfactant for enhanced oil recovery (EOR) applications provided by Shell Oil Company. The molecular structure of an APS courtesy is shown in Fig. 1. It is a negatively charged alcohol alkoxy sulfate surfactant commonly used in EOR with the advantages of excellent divalent ion tolerance and relatively low cost comparing to other type of EOR surfactants. The sulfate surfactant is used without further treatment. Deionized (DI) water system was obtained from the EMD Millipore Corp. (Burlington, MA). The Berea sandstone purchased from Kocurek Industries, Inc. (Caldwell, TX) contains 93% of silica, referred as quartz sand in this paper, was crushed and sieved through 100 and 50 mesh screens to obtain sand grains with diameter between 150 and 300 μm. To obtain the surface charge of the quartz sand grain, 15 g DI-water was agitated with 1.5 g sand grains at room temperature for five minutes. After agitation, the supernatant was taken out and filtered through 0.45 u m syringe filter to remove as much suspended solids as possible. 8 drops of filtered supernatant and 1.25 ml of 1 mM KCl solution were added into the cuvette. NanoBrook Omni was then used to measure the zeta potential, i.e. surface charge, of the mixture in the cuvette. The surface charge of quartz sand grains in DI water was measured as −70 mV. All other chemicals used in these experiments were purchased from Sigma-Aldrich, including branched polyethylenimine (PEI) (average MW: 25,000 g/mol), sodium borate ($Na_2B_4O_7$), methylene blue (MB) ($C_{16}H_{18}N_3SCl$), hyamine ($C_{27}H_{42}ClNO_2$), and chloroform ($CHCl_3$).

2.2. Equipment

The NanoBrook Omni nanoanalyzer (Brookhaven Instruments Corp., Holtsville, NY) was used to measure the particle sizes and zeta potentials of the PECs. A total organic carbon/total nitrogen (TOC/TN) analyzer (Shimadzu Corp., Kyoto, Japan) including TOC-L, TNM-L, and autosampler ASI units, was used to measure the PEI and surfactant concentrations. The quartz crystal microbalance with dissipation (QCM-D) (Biolin Scientific, Linthicum Heights, MD) was utilized to monitor the real-time adsorption of chemical species.

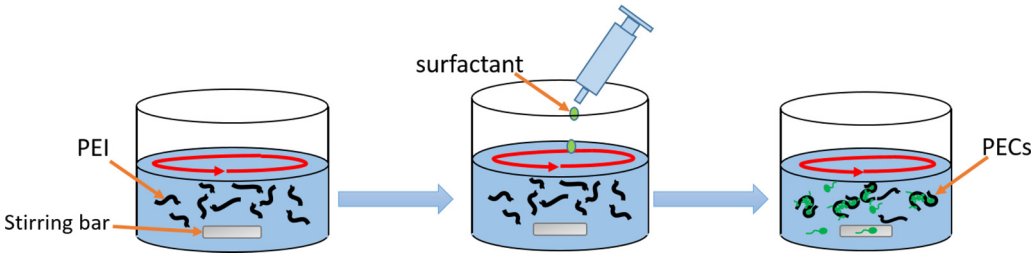

Fig. 2. Schematic procedure of PEC nanoparticle preparation.

2.3. Optimization of PEC recipe

The PEC nanoparticles used this study are formed by complexing cationic PEI with anionic sulfate surfactant, which is the same surfactant used in the adsorption tests. PEC recipes were optimized by altering surfactant and PEI stock solution concentrations, surfactant to PEI weight ratios, and pH of PEI solution. (PEI pH is adjusted by 12N and 4N HCl to the desired pH.) Based on the optimization results, a stable PEC system was produced from a 1 wt% sulfate surfactant solution and 1 wt% PEI solution (pH = 7) mixed in a 1:1 ratio. This recipe was selected for further adsorption studies.

2.4. Preparation of PEC

Stock solution of PEI were prepared with DI water (18.2 MΩ cm at 25 °C). To make PEC nanoparticles, the PEI stock solution was first weighed in a glass beaker, and a magnetic stir bar was added. The preweighed surfactant solution was then rapidly delivered to the vortex of the PEI solution, rotating at 1200 rpm, using a syringe with needle. A schematic of the PEC preparation is shown in Fig. 2. The nanoparticles were then characterized for size and zeta potential as described below. Adsorption experiments were carried out with no further PEC purification.

2.5. Surfactant entrapment efficiency (EE) measurement

Surfactant EE of PEC formulation is defined as the ratio of surfactant concentration entrapped in the PEC to the total surfactant concentration in the PEC suspension. EE can be calculated using the following formula:

$$EE\ (\%) = \frac{(C_{initial} - C_{supernatant})}{C_{initial}} \times 100\% \quad (1)$$

where $C_{initial}$ represents the initial surfactant concentration before the formation of PEC, and $C_{supernatant}$ refers to the concentration of the free surfactant in solution after PEC formation.

To obtain the concentration of free surfactant, the sample was first centrifuged at 14,800 rpm for 90 min to separate PEC nanoparticles from the free PEI and surfactant molecules. Then, a titration was performed using a methylene blue (MB) indicator to measure the concentration of free surfactant. The titration method was modified from one developed by S. R. Epton [29]. The modified method is as follows: 2 mL of PEC supernatant is pipetted into a 20 mL vial. 2 mL of DI water and 50 µL of stabilized MB solution (0.1 g of MB dissolved in 100 mL of 10 mM borate buffer, pH 7–7.5) are added followed by 5 mL of chloroform. 4 mM cationic hyamine is used as the titrant and is added drop wise to the mixture. After each small addition of titrant, the mixture is shaken then kept still for one minute. Before the titration, the blue color concentrates in the lower organic layer because of the formation of surfactant-MB pair. (See Fig. 3 for the principle of the MB titration method.) As the titration proceeds, the surfactant and MB molecules separate due to the formation of a surfactant-hyamine complex. The separated MB molecules then transfer to the upper aqueous layer, carrying with them the distinctive blue color. The end point is achieved when both layers show the equivalent shade of blue. Finally, the sulfate surfactant concentration is calculated using the following equation:

$$C_{surfactant}\ (\%) = \frac{V_{hyamine}\ (\text{mL}) \times 4 \times 10^{-3}(M)\ \times MW_{surfactant}\left(\frac{\text{g}}{\text{mol}}\right)}{2\,\text{mL}\ \times\ 1000} \times 100\% \quad (2)$$

where $C_{surfactant}$ represents the volumetric surfactant concentration, $V_{hyamine}$ is the volume of hyamine spent during the titration process, $MW_{surfactant}$ refers to the molecular weight of sulfate surfactant, which is 700 g/mol, $4 \times 10^{-3} M$ refers to the molar concentration of hyamine, and 2 mL in the denominator of Equation (2) represents the initial volume of sulfate surfactant solution. Equation (2) assumes a hyamine solution density of 1 g/mL and includes a factor of 1000 for unit conversion.

Surfactant EE of the PEC formulation used in this study was determine to be 77 ± 2% using the MB titration method, which means that ~ 23% of the surfactant used to make PEC nanoparticles was not entrapped and remained free in the PEC suspension.

2.6. Characterization of PEC

Particle size and zeta potential of the PEC nanoparticles were measured using the Nanobrook Omni nanoanalyzer. Samples were prepared for particle size measurement by diluting 4 drops of PEC suspension to 3 mL with DI water. The measurements were performed in triplicate at a scattering angle of 90°. For zeta potential measurements, 1.25 mL of 1 mM KCl solution was mixed with 8 drops of sample suspension. The Smoluchowski approximation was then used to calculate the zeta potential of the PEC. The average size of the optimized PEI/surfactant PEC was 138 ± 2 nm while the average zeta potential was +80 ± 7 mV.

2.7. Static adsorption test

Static adsorption tests, using the sulfate surfactant solution and PEC suspension, were performed to evaluate the behavior and mechanism of analyte adsorption. This is accomplished by adding 15 g DI water diluted sample suspension to 1.5 g crushed and sieved (100 and 50 mesh screen) quartz sand grains. The mixture is then shaken at 220 rpm on a benchtop shaker until the adsorption is complete. At the end of the test, the supernatant is aspirated and filtered through a 0.45 µm nylon syringe filter. Concentrations of the surfactant and PEI in the supernatant are measured using the TOC/TN analyses. The percent adsorption of each material is then calculated using Equation (3).

$$\text{Adsorption}\ (\%) = \frac{C_{tot} - C_{after}}{C_{tot}} \times 100\% \quad (3)$$

where C_{tot} represents total concentration of the material added to the PEC suspension, and C_{after} is the concentration of the material remaining in solution after the adsorption test.

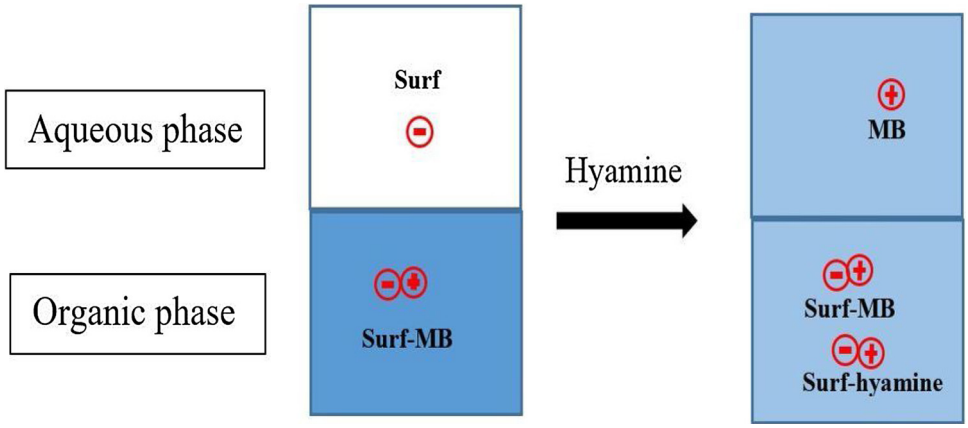

Fig. 3. Schematic illustration of the MB titration method. Surf represents surfactant and MB represents methylene blue.

2.8. PEI and surfactant concentration measurements by TOC/TN

After collecting the samples from the static adsorption tests, the concentrations of the PEI and surfactant in the supernatants were determined using a TOC/TN analyzer. The PEI concentration was measured first by running a total nitrogen (TN) analysis on an aliquot of sample and comparing the result to standard solutions. This procedure is selective for PEI as it is the only molecule in the system that contains atoms of nitrogen. The sample is then subjected to the total organic carbon (TOC) test to determine the TOC of the system (containing both PEI and surfactant). The organic carbon content pertaining to PEI can be calculated from the PEI concentration determined above using TN analysis. Finally, the organic carbon content contributed by the surfactant can be calculated by subtracting the organic carbon attributable to PEI from the TOC of the whole sample.

2.9. Real-time adsorption by QCM-D

Real-time adsorption of sulfate surfactant and PEC were measured by QCM-D. A negatively charged silicon dioxide sensor was used as the analog to quartz sand grains. The procedure is performed as follows: 1) the sensor is flushed with DI water at a 150 μL/min rate to establish a baseline; 2) 0.5 wt% sulfate surfactant solution or a 50 fold dilution of PEC suspension is then pumped over the sensor until the frequency and dissipation of the system reach an equilibrium; 3) the flow is stopped and the system is allowed to incubate under static conditions for a given amount of time to observe adsorption; 4) the sensor is again rinsed with DI water to flush out suspended molecules in the bulk solution and loosely bound materials. After the injection sequence is complete, the frequency shifts (Δf) and dissipation shifts (ΔD) are compared and analyzed qualitatively.

3. Results and discussion

3.1. Hypothesis & proposed adsorption mechanism

We hypothesize that a cationic PEC layer formed on the negatively charged quartz surface can enhance the adsorption of anionic surfactants on quartz sand grains. Based on our hypothesis, we propose a four-stage adsorption mechanism for the enhanced adsorption of anionic surfactants on negatively charged quartz sand grains coated with PEC nanoparticles (Fig. 4). First, the positively charged PEC nanoparticle suspension comes into contact with negatively charged quartz sand grains (Stage I). Then, a large number of PEC nanoparticles [+] and a small amount of free PEI [+] in the nanoparticle suspension will be adsorbed onto the negatively charged quartz sand grains (Stage II). At this point, the sand grains will be coated with a layer of positively charged PEC nanoparticles and a small amount of free PEI. Then, as proposed by Ondaral et al. [25], the adsorbed PEC may undergo a distortion on the surface resulting in increased surface area and charge density. This base layer can then attract and adsorb more free anionic surfactants by charge attraction (Stage III) and through hydrophobic interactions forming a surfactant bilayer (Stage IV) before reaching a new equilibrium. In the following sections, results from static adsorption and QCM-D studies will be used to test the hypothesis and confirm the proposed mechanism for the enhanced anionic surfactant adsorption on quartz sand grains coated with PEC nanoparticles.

3.2. Adsorption of sulfate surfactant on quartz sand grains

3.2.1. Static adsorption test

Static adsorption tests were performed to determine the level of adsorption of anionic surfactants onto negatively charged quartz sand grains. Using the procedure described in Section 2.7, surfactant concentrations in the supernatant were measured at intervals of 6, 12, 24, and 48 h. Results summarized in Fig. 5 show no significant surfactant adsorption even after 48 h of mixing.

3.2.2. Real-time adsorption monitoring using QCM-D

QCM-D was used to monitor the real-time adsorption of the anionic sulfate surfactant onto a negatively charged silicon dioxide sensor. This sensor was chosen as an analog to quartz sand grains. The surface was prepared by first flushing it with DI water to establish a baseline, followed shortly by injection of the surfactant solution. The system was then incubated under static conditions for a period of time before finally being rinsed with DI water to remove the extra materials not adsorbed on the sensor surface.

The QCM-D raw data with the frequency shift (Δf) and dissipation shift (ΔD) are shown in Fig. 6(a) and (b), respectively. In Fig. 6, small changes in frequency and dissipation observed between the initial water injection and surfactant injection were mainly attributed to differences in viscosity and viscoelasticity between the bulk solutions. They may also be explained by effects of the formation of an electrical double layer between the surface and the bulk solution. The frequency shift (Δf), shown in Fig. 6(a), from approximately 1.5 Hz back to the water baseline after the final flush indicates that little to no surfactant adsorption occurred. These observations are consistent with results from the static adsorption test (Fig. 5) where negligible sulfate surfactant adsorption onto quartz sand grains in DI water was observed.

3.3. Adsorption of PEC [+] on quartz sand grains

3.3.1. Static adsorption tests

A static adsorption test of the as prepared positively charged PEC suspension (with 77% surfactant EE) and the quartz sand grains diluted with DI water was performed at room temperature. An experimental

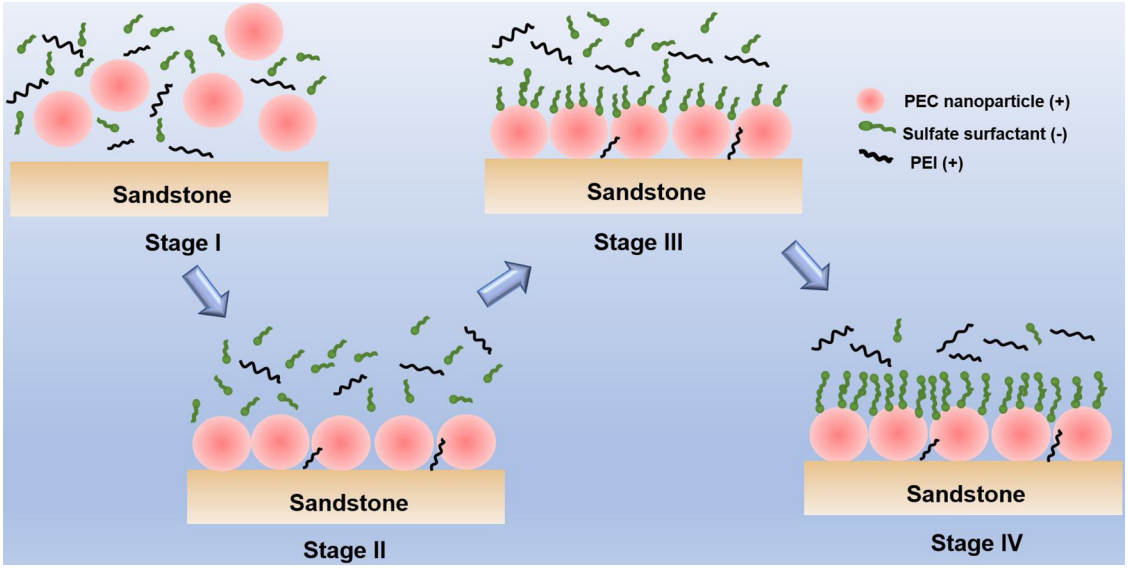

Fig. 4. Schematic representation of surfactant entrapping PEC [+] adsorption on quartz sand grain [−] mechanism.

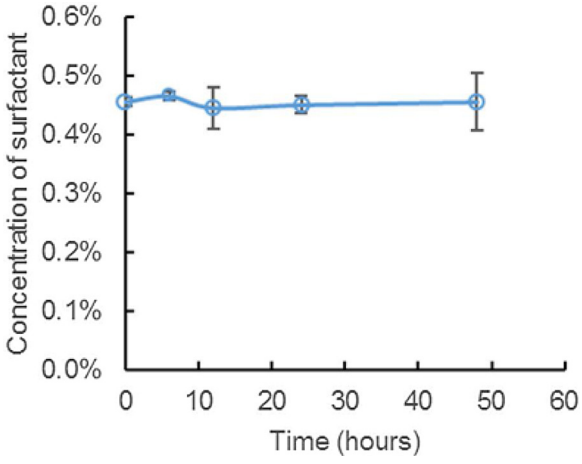

Fig. 5. Concentrations of sulfate surfactant in the supernatant prepared in DI water during the static adsorption test. The initial surfactant concentrations in DI water was 0.45 wt%.

procedure is shown in Fig. 7. Fig. 8(a) plots the sulfate surfactant concentration measured in the supernatant versus the contact time and the corresponding percent surfactant adsorption relative to the amount of total surfactant concentration (both entrapped in PEC & free) originally contained in the diluted PEC/sand sample. As shown in Fig. 8(a), after 48 h of agitation with sand grains, the surfactant concentration in the supernatant decreased from 0.51 wt% to 0.01 wt%, indicating a close to 100% adsorption of all the surfactant originally contained in the PEC suspension. Fig. 8(b) contains images of the supernatant during the static adsorption test. As shown in Fig. 8(b), when the contact time increased from 6 h to 48 h, the PEC suspension changed from opaque to almost transparent, indicating that almost all the PEC nanoparticles were adsorbed onto the quartz sand grains after 48 h of contact time. An aliquot of the supernatant after 48 h of contact time was then taken for particle size measurement using the NanoBrook Omni nanoanalyzer. Results from the measurements showed a very low count rate of 13 kcps, which indicates that nanoparticle concentration in the supernatant was extremely low.

Since the surfactant entrapment efficiency of the PEC is around 77%, it means that close to 23% of the surfactant remains free in the PEC suspension. According to results shown in Section 3.2.1, the level

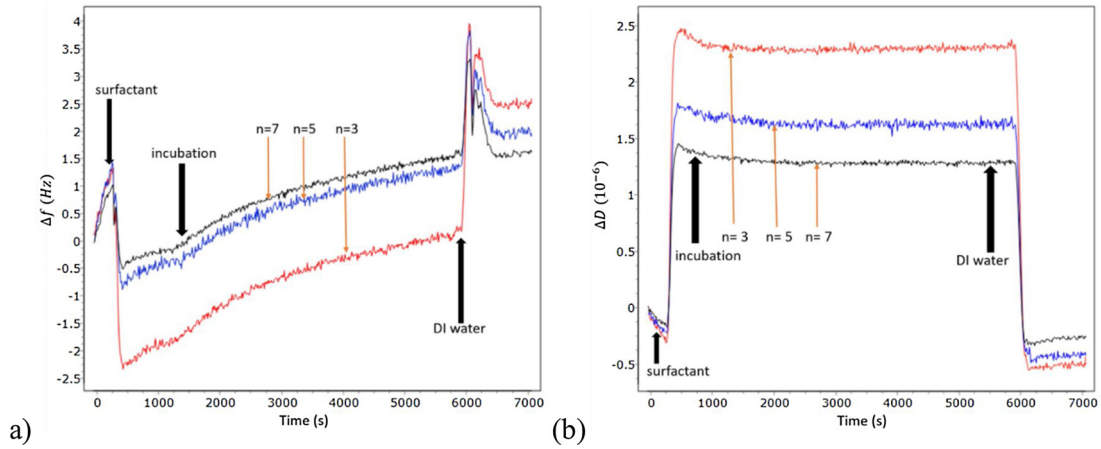

Fig. 6. (a) Frequency shift (Δf) raw data and (b) dissipation shift (ΔD) raw data of sulfate surfactant real-time adsorption on silicon sensor in DI water. Δf and ΔD are measured simultaneously at three different overtones (n = 3, 5, and 7) at 25 °C.

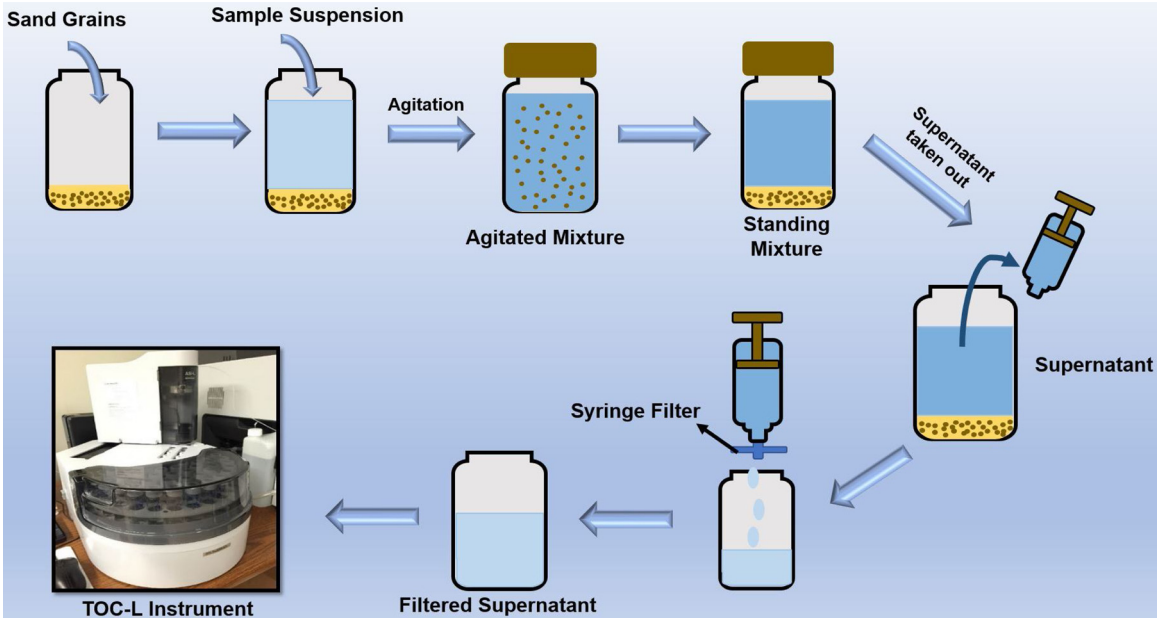

Fig. 7. Schematic illustration of experimental procedure used in static adsorption tests.

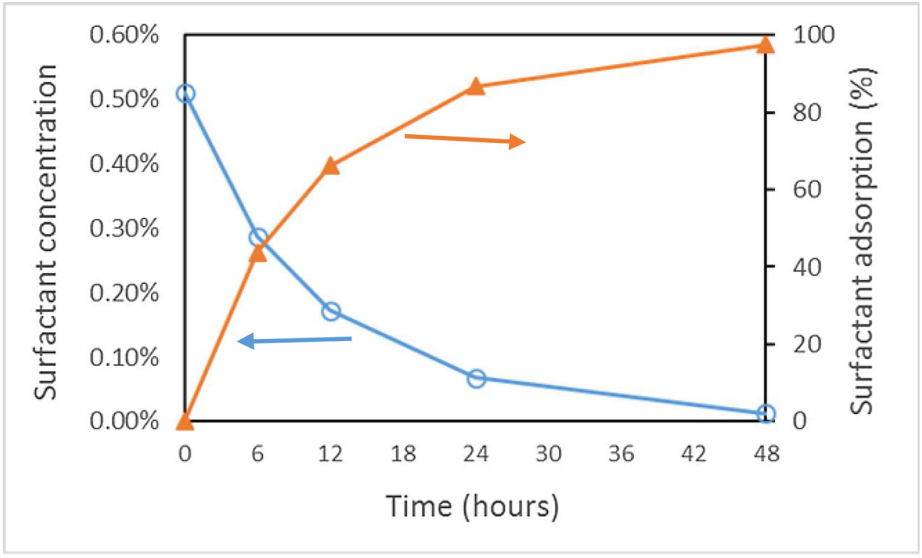

(a)

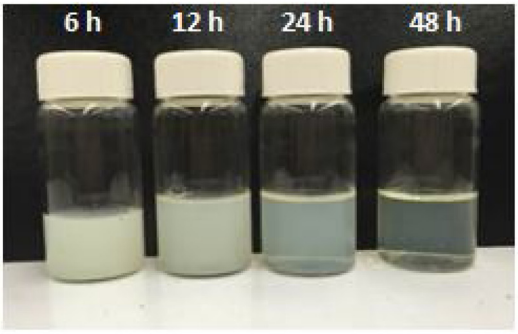

(b)

Fig. 8. (a) Concentrations (wt%) (hallow circle) and adsorption percentage (triangle) of the surfactant in the supernatant after PEC suspension diluted in DI water and agitated with quartz sand grains for different hours. (b) Images of collected supernatants after diluted PEC suspension agitated with quartz sand grains for different time periods.

of sulfate surfactant adsorption on quartz sand grains was extremely low (Fig. 5). That means the unentrapped free anionic sulfate surfactant in the PEC suspension are not supposed to be adsorbed onto the negatively charged quartz sand grains. However, we observed a close to 100% adsorption of the sulfate surfactant (both entrapped and un-entrapped) present in the PEC suspension. These results support our

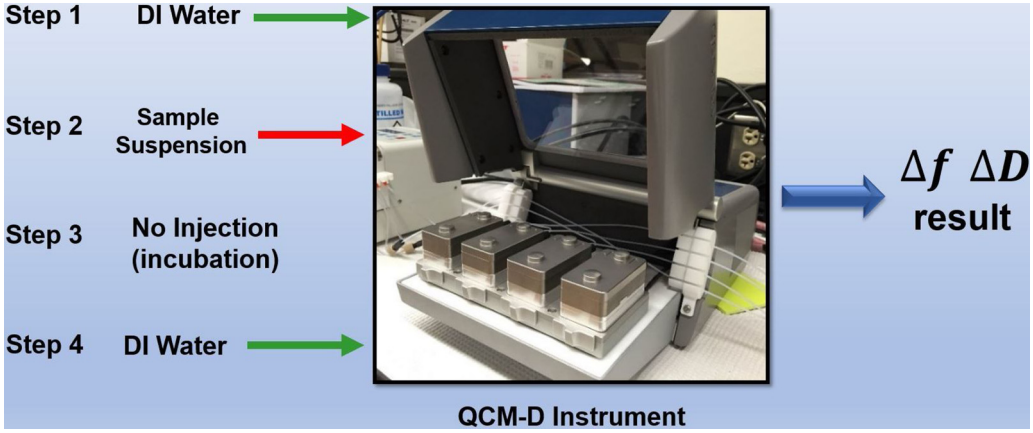

Fig. 9. Schematic illustration of experimental procedure used in real-time PEC adsorption tests using QCM-D.

proposed enhanced surfactant adsorption mechanism (Fig. 4) that, after the adsorption of a large amount of positively charged PECs onto the negatively charged quartz sand grains, the surface charge of the coated sand grains becomes positive, thereby allowing the unentrapped anionic sulfate surfactant to be adsorbed onto the coated quartz sand grains.

3.3.2. Real-time adsorption monitoring using QCM-D

The PEC adsorption onto the silicon oxide sensor in DI water was measured using the QCM-D. The experimental procedure of PEC real-time adsorption tests using QCM-D is illustrated in Fig. 9. The test begins by flushing DI water through the system to establish a baseline. Next, the sensor was flushed with the PEC suspension and left under static conditions to establish the new baseline after the sensor was coated with PEC/PEI. The raw data are shown in Fig. 10. During the PEC flushing period, a decrease in Δf (~ 4.5 Hz) and a comparatively small increase in ΔD (0.25×10^{-6}) were observed, which also accompanied by overlapping overtones. These observations are consistent with formation of a rigid film on the silicon dioxide surface. At this point, we believe that a large amount of the PEC [+] and a small amount of free PEI [+] were adsorbed onto the oppositely charged silica sensor [−] by electrostatic attraction.

DI water was then injected to remove the loosely attached materials on the sensor surface until Δf and ΔD reached an equilibrium. Relatively small changes in Δf (~0.5 Hz) and ΔD observed during this period are consistent with Stage II of our proposed mechanism (Fig. 4) where strong adsorption of the positively charged PEC/PEI occurred on the negatively charged sensor surface with negligible amount of adsorbed PEC/PEI being flushed away during the DI water injection.

At this point, 0.5 wt% sulfate surfactant was pumped onto the PEC/PEI-coated sensor. In this case, the drop in Δf (~12 Hz) was significantly larger than any changes seen from the sulfate surfactant real-time adsorption test on bare silica sensor previously discussed (Fig. 6(a)). This provides convincing evidence of the PEC's ability to promote surfactant adsorption. The significant increase in ΔD (4×10^{-6}) after surfactant injection, coupled with broadening of the overtones, further indicates that a soft and viscoelastic surfactant layer had formed. These observations are consistent with a combination of Stages III and IV (Fig. 4) of the proposed PEC enhanced adsorption mechanism.

3.4. Adsorption of sulfate surfactant on PEC [+] treated vs untreated sand grains

Next, we performed another set of static adsorption tests comparing the adsorption of sulfate surfactant on PEC treated vs. untreated sand grains to quantify the enhanced adsorption capacity and confirm the proposed enhanced adsorption mechanism.

To prepare the PEC treated sand grains, 1.5 g of quartz sand grains were firstly agitated with the surfactant entrapping PEC [+] suspension for two days. Then, the supernatant was aspirated completely from the test vial to remove the non-adsorbed PECs, PEI, and surfactants.

15 g of known concentration of sulfate surfactant solutions (~0.5 wt%) was added to the test vial containing either 1.5 g bare sand grains or the same amount of PEC treated sand grains. The mixtures were then agitated for another 24 h. After the supernatants being centrifuged and filtered, the surfactant concentrations in the supernatants were then measured by TOC/TN and shown in Fig. 11.

For the adsorption test performed with bare quartz sand grains, the surfactant concentration changed from 0.46 wt% to 0.45 wt%,

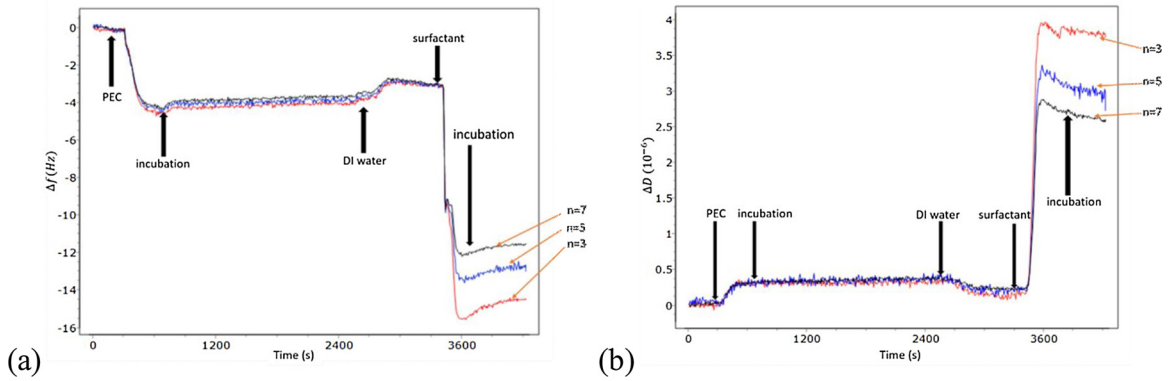

Fig. 10. (a) Frequency shift (Δf) raw data and (b) dissipation shift (ΔD) raw data of PEC real-time adsorption on silicon sensor in DI water. Δf and ΔD are measured simultaneously at three different overtones (n = 3, 5, and 7) at 25 °C.

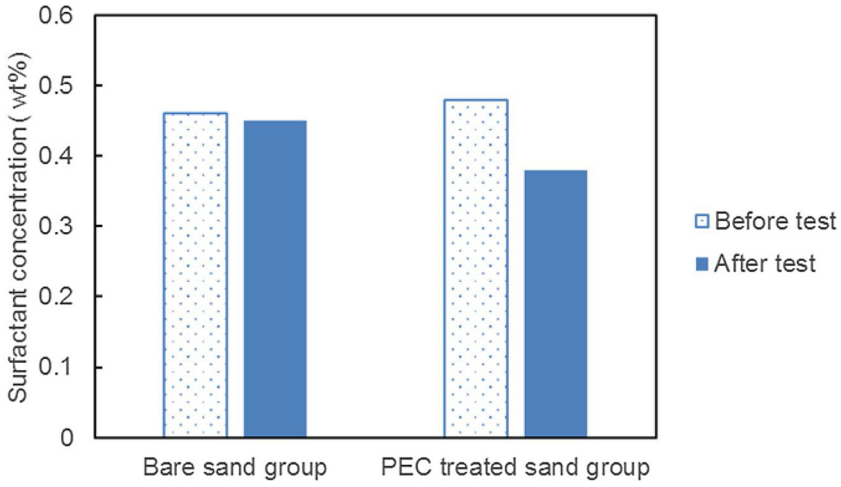

Fig. 11. Sulfate surfactant concentrations in the supernatant before and after 24 h of adsorption tests at room temperature with bare quartz sand grains (left) (initial concentration 0.46 wt% dropped to 0.45 wt% after the test) and PEC-treated quartz sand grains (right) (initial concentration 0.48 wt% dropped to 0.38 wt% after the test).

indicating no apparent sulfate surfactant adsorption (Fig. 11 left). In contrast, for the test using the PEC treated quartz sand grains, surfactant concentration in the supernatant decreased from 0.48 wt% to 0.38 wt% (Fig. 11 right) suggesting that 21% of the surfactant originally in the supernatant was adsorbed onto the sand grains. These results show that treating the negatively charged quartz sand grains with PEC nanoparticles can indeed enhance the adsorption of the anionic sulfate surfactant (Fig. 4, Stage III & IV).

As reported earlier, the surfactant entrapment efficiency of the PEC is around 77%. However, results from Section 3.3.1 indicated that 23% of the free surfactant in the PEC suspension was also completely adsorbed on the PEC treated sand grains during the process. This means that, to determine the overall enhanced adsorption capacity of the PEC treated sand grains, we must also take into account the adsorption of the free unentrapped surfactant in the PEC suspension during the treatment process.

Since the total surfactant concentration in the PEC suspension used to treat the sand grains is 0.5 wt%, with the EE of 77%, the amount of the free unentrapped surfactant in the 15 g of suspension is equal to 0.115 wt% (0.5 wt% × 0.23), which was completely adsorbed. The additional amount of surfactant adsorbed when another 15 g of 0.48 wt % of surfactant solution was added to interact with the treated sand grains is 0.1% (0.48% − 0.38%). So, the total weight of free sulfate surfactant adsorbed onto the treated sand grains is 32.25 mg (15 g × (0.115 + 0.1) wt%). Since 1.5 g of sand treated with PEC was used in the adsorption tests, the total adsorption capacity of the free surfactant is 21.5 mg per gram of sand. This is in contrast to the case for untreated bare sand grains where no apparent adsorption of the anionic sulfate surfactant was observed. These results demonstrate the potential of using PEC nanoparticles to enhance the adsorption of anionic surfactants on negatively charged surface of quartz sand grains and confirmed the proposed mechanism for enhanced surfactant adsorption.

4. Conclusions

i Results from the static adsorption tests showed that the level of adsorption of the anionic sulfate surfactant on PEC treated quartz sand grains (21.5 mg/g of sand) was significantly higher than that on bare untreated sand grains (negligible adsorption).

ii Real-time monitoring using QCM-D (Fig. 10) observed a decrease in Δf (~ 4.5 Hz) and a comparatively small increase in ΔD (0.25×10^{-6}) when the silica sensor (a sandstone analog) was flushed with PEC, which are consistent with formation of a rigid film on the silica oxide sensor surface, indicating the adsorption of the PEC [+] and a small amount of free PEI [+] onto the oppositely charged silica sensor [−] by electrostatic attraction.

iii In contrast, the QCM-D data showed very small changes in frequency and dissipation observed between the initial flushing the quartz sensor with water and the subsequent flushing with surfactant injection. The frequency shift (Δf), shown in Fig. 6(a), from approximately 1.5 Hz back to the water baseline after the final flush indicates that little to no surfactant adsorption occurred.

iv Both static adsorption tests and real-time adsorption monitoring using QCM-D confirmed our hypothesis that a cationic PEC layer formed on the negatively charged quartz surface can enhance the adsorption of anionic surfactants on quartz sand grains.

v Our results also confirmed a proposed four-stage adsorption mechanism for the enhanced adsorption of anionic surfactants on negatively charged quartz sand grains treated with PEC nanoparticles.

Author contributions

The manuscript was written through contributions of all authors. All authors have given approval to the final version of the manuscript.

Funding

This research did not receive any specific grant from funding agencies in the public, commercial, or not-for-profit sectors.

Acknowledgment

The authors would like to thank Shell Oil Company for providing EOR surfactant samples.

References

[1] S. Paria, K.C. Khilar, A review on experimental studies of surfactant adsorption at the hydrophilic solid–water interface, Adv. Colloid Interface Sci. 110 (2004) 75–95.
[2] Y. Wang, H. Xu, W. Yu, B. Bai, X. Song, J. Zhang, Surfactant induced reservoir wettability alteration: recent theoretical and experimental advances in enhanced oil recovery, Pet. Sci. 8 (2011) 463–476.
[3] D. Levitt, A. Jackson, C. Heinson, L.N. Britton, T. Malik, V. Dwarakanath, G.A. Pope, Identification and evaluation of high-performance EOR surfactants April, SPE Reservoir Evaluation & Engineering (2009) SPE 100089.
[4] S.B. Sandersen, Enhanced Oil Recovery with Surfactant Flooding, PhD dissertation in Department of Chemical and Biochemical Engineering Technical University of Denmark, 2012.
[5] P. Somasundaran, L. Zhang, Adsorption of surfactants on minerals for wettability control in improved oil recovery processes, J. Pet. Sci. Technol. 52 (2006) 198–212.
[6] J.T.I. Penfold, J. Petkov, R.K. Thomas, Surfactant adsorption onto cellulose surfaces, Langmuir 23 (2007) 8357–8364.
[7] S.B. Alila, M.N. Belgacem, D. Beneventi, Adsorption of a cationic surfactant onto cellulosic fibers I. Surface charge effects, Langmuir 21 (2005) 8106–8113.
[8] D.A. Nieto-Alvarez, L.S. Zamudio-Rivera, E.E. Luna-Rojero, D.I. Rodríguez-Otamendi, A. Marín-León, R. Hernández-Altamirano, V.Y. Mena-Cervantes, T.D. Chávez-Miyauchi, Adsorption of zwitterionic surfactant on limestone measured with high-performance liquid chromatography: micelle–vesicle influence, Langmuir 30 (2014) 12243–12249.

[9] X. Zhang, B. Chen, W. Dong, W. Wang, Surfactant adsorption on solid surfaces: recognition between heterogeneous surfaces and adsorbed surfactant aggregates, Langmuir 23 (2007) 7433–7435.
[10] M.J. Rosen, Surfactant and Interficial Phenomena, third edition, A John Willey & Sons, INC., Indianapolis, 2004.
[11] A.P. Robertson, J.O. Leckie, Cation binding predictions of surface complexation models: effects of pH, ionic strength, cation loading, surface complex, and model fit, J. Colloid Interface Sci. 188 (1997) 444–472.
[12] O.S. Pokrovsky, J. Schott, F. Thomas, Dolomite surface speciation and reactivity in aquatic systems, Geochim. Cosmochim. Acta 63 (1999) 3133–3143.
[13] J.L. Salager, Surfactants Types and Uses, (2002) http://www.nanoparticles.org/pdf/Salager-E300A.pdf.
[14] S. Che, A.E. Garcia-Bennett, T. Yokoi, K. Sakamoto, H. Kunieda, O. Terasaki, T.A. Tatsumi, Novel anionic surfactant templating route for synthesizing mesoporous silica with unique structure, Nat. Mater. 2 (2003) 801–805.
[15] J. Berger, M. Reist, J.M. Mayer, O. Felt, R. Gurny, Structure and interactions in chitosan hydrogels formed by complexation or aggregation for biomedical applications, Eur. J. Pharm. Bio-Pharm. 57 (2004) 35–52.
[16] C. Zaino, Y. Zambito, G. Mollica, M. Geppi, M.F. Serafini, V. Carelli, G.D. Colo, A novel polyelectrolyte complex (PEC) hydrogel for controlled drug delivery to the distal intestine, Open Drug Dev. J. 1 (2007) 68–75.
[17] S. Lankalapalli, V.R.M. Kolapalli, Polyelectrolyte complexes: a review of their applicability in drug delivery technology, Indian J. Pharm. Sci. 71 (2009) 481–487.
[18] R. Barati, S.J. Johnson, S. McCool, D.W. Green, G.P. Willhite, J.T. Liang, Fracturing fluid cleanup by controlled release of enzymes from polyelectrolyte complex nanoparticles, J. Appl. Polym. Sci. 121 (2011) 1292–1298.
[19] R. Barati, S.J. Johnson, S. McCool, D.W. Green, G.P. Willhite, J.T. Liang, Polyelectrolyte complex nanoparticles for protection and delayed release of enzymes in alkaline pH and at elevated temperature during hydraulic fracturing of oil wells, J. Appl. Polym. Sci. 126 (2012) 587–592.
[20] M. Cordova, M. Cheng, J. Trejo, S.J. Johnson, G.P. Willhite, J.T. Liang, C. Berkland, Delayed HPAM gelation via transient sequestration of chromium in polyelectrolyte complex nanoparticles, Macromolecules 41 (2008) 4398–4404.
[21] S.J. Johnson, C. Berkland, A. Moradi-Araghi, J.T. Liang, T.M. Christian, R.B. Needham, M. Cheng, Y.Y. Lin, A.B. Woodside, Low Molecular Weight Polyacrylates for EOR, US Patent, US2016/0115371 A1, 2016.
[22] Y.Y. Lin, C. Berkland, C.J.T. Liang, A. Moradi-Araghi, T.M. Christian, R.B. Needham, J.H. Hedges, M. Cheng, F.L. Scully, D.R. Zornes, Delayed Gelling Agents, US Patent, US2014/0209305A1, 2014.
[23] T. Reihs, M. Müller, K. Lunkwitz, Deposition of polylelectrolyte complex nanoparticles at silica surfaces characterized by ATR-FTIR and SEM, Colloids Surf. A: Physicochem. Eng. Asp. 212 (2003) 79–95.
[24] T. Reihs, M. Müller, K. Lunkwitz, Preparation and adsorption of refined polyelectrolyte complex nanoparticles, J. Colloid Interface Sci. 271 (2004) 69–79.
[25] S. Ondaral, C. Ankerfors, L. Ödberg, L. Wågberg, Surface-induced rearrangement of polyelectrolyte complexes: influence of complex composition on adsorbed layer properties, Langmuir 26 (2010) 14606–14614.
[26] M.Y. Arteta, F. Eltes, R.A. Campbell, T. Nylander, Interactions of PAMAM dendrimers with SDS at the solid–liquid interface, Langmuir 29 (2013) 5817–5831.
[27] Y. Gao, Fundamental Studies of Refined Polyelectrolyte/Surfactant Nanoparticles Bulk and Interfical Properties, PhD Dissertation, Department of Chemical and Petroleum Engineering, University of Kansas, 2014.
[28] Y. Gao, L.T. Duc, A. Ali, B. Liang, J.T. Liang, P. Dhar, Interface-induced disassembly of a self-assembled two-component nanoparticle system, Langmuir 29 (2013) 3654–3661.
[29] S.R. Epton, A rapid method of analysis for certain surface-active agents, Nature 160 (1947) 795–796.